

Observations
of the
CALIFORNIA INSTITUTE OF TECHNOLOGY
RADIO OBSERVATORY

Owens Valley, California

1962

1. BRIGHTNESS DISTRIBUTION IN DISCRETE RADIO SOURCES
III. THE STRUCTURE OF THE SOURCES

by
P. Maltby and A. T. Moffet

BRIGHTNESS DISTRIBUTION IN DISCRETE RADIO SOURCES
III. THE STRUCTURE OF THE SOURCES

by

P. Maltby and A. T. Moffet

California Institute of Technology
Radio Observatory

Owens Valley, California

ABSTRACT

The visibility functions of 195 radio sources are interpreted in terms of the structure of these sources. Of the 195 sources, 174 are known or presumed to be extragalactic. Seventy-five of these extragalactic sources are resolved with the interferometer spacings used, and complex structure is found in all but 13. In the sources showing complex structure, two similar components with nearly equal intensities are found in 15, 40 show two or more components of unequal intensities, while 7 appear to be a bright core surrounded by a halo. It is suggested that the majority of all extragalactic sources have complex structure.

Data are also given on the brightness distributions in the 21 galactic sources observed. In contrast to the extragalactic sources, emission from the galactic sources is typically confined to a single region.

I. INTRODUCTION

In the two preceding papers, we have presented data on the visibility functions of 195 discrete radio sources observed at 31.3 cm with the Caltech variable spacing interferometer. The first paper (Moffet 1962, hereafter referred to as Paper I) reported measurements on 127 sources observed with an east-west interferometer baseline, while the second (Maltby 1962, Paper II) reported similar measurements on 165 sources using a north-south baseline. Ninety-seven sources were included in both sets of observations.

In the present paper we report the interpretation of these data in terms of the brightness distributions of the sources. The methods of interpretation are set forth, and the source descriptions are given in Tables 1 and 4. Finally, some conclusions about source structure are drawn. A detailed study of the implications of these results for 25 identified sources will be given in the fourth paper of this series (Maltby, Matthews, and Moffet 1962).

II. METHODS OF INTERPRETATION

The definition of the visibility function of a source and the relation of the visibility function to the source brightness distribution have been given in Paper I. We recall that the visibility function is proportional to the complex, two-dimensional Fourier transform of the source brightness distribution. Thus, if the visibility function were known in its entirety, the complete brightness distribution could be recovered by a numerical Fourier inversion. When the visibility function is not completely determined by the observations (as is almost always the case), a Fourier inversion of the known portion of the visibility function yields an approximation to the source brightness distribution. This approximation is known as the principal solution (Bracewell and Roberts 1954).

An alternative method of interpreting the visibility function is to compare that portion which has been observed with artificial visibility functions calculated for a number of plausible source models. Parameters in a particular model are then adjusted to give a best fit to the observed data for a given source, and the source is described in terms of the fitted model.

Both methods of analysis have been used in making the interpretations reported in this paper, and a description of our procedures follows.

a) Fourier Inversion

For all the galactic sources, and for a number of the larger extragalactic sources, the east-west and north-south one-dimensional visibility functions (given in Papers I and II) were numerically inverted using an electronic digital computer. The inversion was done by evaluating a Fourier series, a process which is much simpler than numerically calculating a Fourier integral, and which gives identical results for sources which are of limited angular extent.

To obtain, by this method, the one-dimensional brightness distribution of a source, the observed values of the visibility amplitude for the source were first plotted as functions of the antenna spacing. A smooth curve was steered as nearly as possible through the points. This procedure was then repeated for the visibility phase. The values of these curves were read off at equal intervals of antenna spacing, and these numbers were inserted as coefficients and phase-shifts in the Fourier series representing the source. For sources observed with both the east-west and the north-south baselines, separate one-dimensional inversions were made of each set of data.

Because the observations were not taken at equal intervals of antenna spacing, the values obtained from the curves and fed into the Fourier series were not completely determined by the observations. Where there were alternative interpolations of equal plausibility, different series were evaluated and the one which gave the most reasonable source distribution was accepted to represent the source. In this sense, "most reasonable" usually meant the distribution with the least amount of negative brightness.

In the cases where the spurious responses in the principal solution were evident, the recovered distribution was smoothed with a Gaussian having a full-width at half-maximum of 1.8. This smoothing was accomplished by multiplying the visibility amplitude by the appropriate Gaussian tapering function and transforming the product. The corresponding "beamwidth" for the untapered 1557 wavelength aperture is 1.3.

b) Model Fitting

Most of the extragalactic sources were only partially resolved at the greatest antenna spacings available. For these sources, the method of Fourier inversion was unsuitable since the oscillatory nature of the principal solution obscured the few features of the source distribution which were determined by the observational data. For these sources, the method of model fitting proved much more satisfactory.

In this method, the observed data on the visibility amplitude and phase were compared with artificial visibility functions calculated for a number of physically reasonable models. Free parameters in an appropriate model were then adjusted to give a fit to the observed data. Because of the uncertainty in the data, an adequate fit could be obtained for a range of values of the model parameters, and this range was noted.

The advantage of this method is that it eliminates the problem of the oscillations in the principal solution and gives a recovered source distribution (the model) which is ab initio physically reasonable. The possible differences between the source and the model should be kept in mind, however. Their only relationship is that they have, within the limits of observational error, the same principal solution. The accuracy with which the model represents the source is then dependent upon the degree of resolution. A barely-resolved source can be fitted by any model having the same second moment as does the source (see Paper I, section IIId). Only an equivalent diameter is quoted for such sources. This is the diameter at half-intensity of the equivalent circular Gaussian model, the simplest model that can be chosen. It is probable that in most such cases this simple model does not correspond very well to the true shape of the source.

For a source having a larger angular extent, a more detailed description is possible, and a more complicated model is usually required to fit the observed portion of the visibility function. In many cases a model with two Gaussian components gives a good fit. It should be mentioned that in addition to the one- and two-component Gaussian models, a number of other types of more complicated models were also calculated. In no case were our data sufficient to define a model with more than two components, but in relatively few cases were there indications of a greater degree of complexity.

In a large number of cases it is possible to say with considerable certainty that the two-component model is a good representation of the major features of the source. Certainly some structure within the components is to be anticipated. Nevertheless, many sources are definitely characterized by two well-separated regions of emission--that is to say, two bright areas with a relatively dark region in between.

c) Examples

As an example of the alternative methods of interpretation of the visibility function consider the source 3C 353, which was observed only with the east-west baseline. Because the declination of this source is virtually zero, the fringe rotation is negligible for the east-west observations made off-transit, and all the east-west observations can be combined to give the visibility function for¹ $p = 90^\circ$. The data, from Paper I, on the visibility amplitude is plotted in Figure 1a; that on the phase is plotted in Figure 1b.

The curves in Figures 1a and b were used as the input data for a numerical Fourier inversion. The phase curve shown gave a more satisfactory result than did one running through the centers of the observed points. The result, given in Figure 1c, is the principal solution for this source as observed with a 1600 wavelength aperture. The extraneous responses are clearly evident. The first negative response from each component falls on the nearer side of the other component; thus, the apparent spacing of the two components, as obtained by this method, is too great.

In Figure 1d is shown the result of smoothing the principal solution for 3C 353 with a 1.8 Gaussian. The strong "sidelobes" have vanished but the dip between the components has been filled in.

A model consisting of two Gaussians having equal diameters of 1.4, relative intensities of 2.0 and 1, and an east-west spacing of 2.5 is shown in Figure 1e. The same model, smoothed with a 1.8 Gaussian, is shown in Figure 1f. The visibility amplitude and phase for this model are compared with the observed data for 3C 353 in Figures 1g and h. The fit in amplitude is quite good. The fit in phase could be improved by assigning a slightly smaller diameter to the stronger component.

As another example of model fitting, consider the source 3C 219, which has been observed in three different position angles: $p = 0^\circ$, $p = 53^\circ$ and $p = 90^\circ$. The visibility curves show a pronounced second maximum, and the phase observed in $p = 0^\circ$ at the longest antenna spacing differs by 180° from the phase observed at the shorter spacings. This information suggests that we may try to fit the observations with a model consisting of two equal components. The model which gives the best fit has two equal Gaussian components with diameters of 0.85. The major axis of the source is in position angle 35° and the separation between the components is 1.9. The model source is shown in Figure 2a, while the calculated visibility curves may be compared with the observed visibility amplitudes in Figure 2b.

The source 3C 134 was observed in $p = 0^\circ$, 46° and 90° . Although it has a very small extent in $p = 90^\circ$, observations in the other direction clearly show it to be double. It was found, however, that the observed points could not be fitted to visibility curves for a model source with circular components. A good fit could be obtained if the components were elongated in the direction of the major axis.

¹As in Papers I and II, p is the position angle, defined in the conventional sense.

The resulting model and the fit obtained are shown in Figures 3a and b.

III. THE ORIENTATION OF THE SOURCES

Many sources were found to have two components or to be otherwise elongated. For each such source an effort was made to determine the orientation of its major axis. In many cases the position angle of the major axis could be deduced from the visibility functions obtained with two or more different baseline orientations. Examples of this type of analysis are 3C 219 and 3C 134, which have been described above.

For three sources of particular importance (NGC 5128, Hercules A, and Cygnus A), additional observations were undertaken in June, 1961, to establish more precisely their orientation. The method used was that demonstrated by Jennison and Latham (1959) and by Rowson (1959). The two elements of the Caltech interferometer were placed 1600 ft apart along a north-south baseline. Using a wavelength of 21.7 cm, each source was tracked for a period of four to eight hours. During this period the orientation of the source with respect to the interference fringes changed appreciably. The apparent intensity of the source as a function of hour angle then gave considerable information about the orientation and structure of the source.

The observations for Hercules A are shown in Figure 4a. From the east-west and north-south transit observations, it was known that this source had two components and that the position angle of the major axis was not far from 90° . The expected intensity as a function of hour angle was calculated for a number of model sources. A good fit to the observed data was given by a model having two circular Gaussian components with relative intensities of 1.4 and 1, separated by 1.95 along an axis in $p=100.95$. The component diameters were 0.75 . The curve in Figure 4a is calculated for this model. The deviations from the observed points are small, indicating that the components of Hercules A are nearly circular in shape. The expected east-west visibility amplitude is plotted in Figure 4b together with the observed points. Here again, a good fit is found.

Similar data for Cygnus A is plotted in Figure 5. The position angle of the major axis was found to be 109.0 ± 1.95 , in agreement with the observations of Rowson (1959) at 10 cm. A slight discrepancy was found between the observed and calculated intensities for hour angles between 3^h and 4^h . This suggests that the components may be somewhat elongated in the direction of the major axis.

A study of NGC 5128, using this technique, has been reported separately (Maltby 1961). In this case the components of the source are definitely elongated, and in a direction approximately along the major axis.

IV. INTERPRETATION

The data on the source visibility functions have been interpreted in terms of source structure, using the methods described above. For purposes of classification, it is convenient to treat separately those sources known or presumed to be of galactic origin. Small-diameter objects ($<3'$) with normal, non-thermal spectra have been included in the extragalactic group, even when found at low galactic latitudes. The source 3C 48 has been placed in the galactic group on the basis of its identification with a stellar object (Sandage, Greenstein, Munch, and Matthews, in preparation).

a) Table of Extragalactic Sources

Table 1 contains the interpretations for 17⁴ sources believed to be of extragalactic origin. The sources are listed in order of right ascension and are identified by their numbers in various catalogs¹. In some cases angular diameters in $p = 90^\circ$ and $p = 0^\circ$ have been assigned on the basis of the east-west and north-south transit observations. These diameters refer to circular Gaussian models. Where the observations indicated a complex structure, to which a simple diameter could not be assigned, a 'c' is entered in the appropriate diameter column, and the interpretation of the source is given in the comments. An asterisk indicates a source for which a more extended remark is given in the text (next section). Where observations were made with only one baseline orientation, a dash is entered in the other diameter column. Most of the dimensions quoted for the sources are accompanied by limits. These are based on the range of the model parameters over which the model would give a satisfactory fit to the observed visibility function. The probability that the dimensions of the major features of a source lie within the quoted range is estimated to be about 70%.

As the information in Table 1 was being assembled, it became clear that the extragalactic sources could be divided according to structure into several classes. First of all, many sources were unresolved, or only slightly resolved, with the longest baseline used. For such a source, only a diameter, or an upper limit on a diameter, was determined. Sources having diameters greater than 1.5 were large enough for structural details to be apparent with the baselines available. For a few of these larger sources, the visibility curve showed a smooth decline in amplitude to nearly zero with negligible phase shift. These few sources were fitted with single-component Gaussian models.

As was mentioned above, in the section on model fitting, the majority of the well-resolved sources have more complicated structures. Many contain two, roughly symmetrical components. Others contain two components of unequal intensity. A few sources display a small-diameter core superposed on a large-diameter halo. The classification of a source within these structural categories is indicated in Table 1 by a letter, as follows:

N--not resolved, or only barely resolved.

S--simple; diameter > 1.5 , but no indication of structure.

E--two components of roughly equal intensity; intensity ratio $< 1.4:1$.

U--two components of unequal intensity; in a few cases more complex structure is possible, as noted in the comments.

H--core superposed on halo.

Where the classification is uncertain, the letter is enclosed in parentheses.

The information in Table 1 should not be used without some regard for the way in which it was derived. The accuracy of the descriptions

¹For detailed references, see Paper I, Section IV.

is limited by the small number of antenna spacings used and by the limited accuracy of the measurements of the visibility function, especially of the visibility phase. To cite an example, a number of sources are described as having two components of equal diameters and of unequal intensities. For many of these sources it would also be possible to have unequal component diameters with a slightly different ratio of intensities. The distinction between these possibilities can only be made with accurate measurements at longer baselines. The equal-diameter model has been chosen for simplicity, but the uncertainty has been considered in assigning error limits to the diameters and the intensity ratios, which appear in Table 1. As another example, a faint, large-diameter halo around a source could easily have been missed if no total power measurement were available. In spite of the possibility of such errors, it is felt that wherever a description is given it is a valid description of the major features of the source distribution.

b) Remarks on Individual Extragalactic Sources

Several sources require more extensive comments than could be given in Table 1, and these are given here. In most cases these remarks involve comparison of the present results either with information about an associated optical object or with radio information obtained at other wavelengths.

MSH 00-222 (NGC 253).--Radio emission from NGC 253 was first noted by Mills (1955). The present observations suggest a source having two components with a separation of about 3' in the north-south direction. It is interesting to note that in NGC 253 there is an emission patch 2.3 north of the nucleus (Humason, Mayall, and Sandage 1956).

NGC 1275.--A very extended structure in this source ($\sim 0.5 \times 1.0$) has been observed by Leslie and Elsmore (1961) at a wavelength of 1.68 m. The antenna spacings used in the present study were taken at intervals too great to permit the description of a source of this size; therefore, the interpretation in Table 1 may be in error, but it is also possible that the halo is weaker at shorter wavelengths.

Fornax A.--This source is also too large for the antenna spacings available in the present study. The unequal, two-component structure was discovered by Wade (1961) in observations with a 16' pencil beam at 10-cm wavelength. Similar observations have been made at this Observatory, yielding results which agree fully with those of Wade. The very small visibility amplitudes observed for Fornax A in the present study suggest that the individual components of the source do not contain bright cores of small angular diameter.

3C 134.--The source consists of two components of equal intensity. One or probably both components are elongated approximately in the direction of the major axis of the source (see Figure 3). In this respect 3C 134 is similar to the central component of Centaurus A.

Pictor A.--This source is highly elongated and may consist of two equal components with a separation of 4.6 ± 0.5 in $p = 90^\circ$ and with component diameters of about 2'. The diameter in the north-south direction is $< 2'$. The phase observed at the 779 λ spacing in the east-west direction does not agree with this interpretation, however, and this may indicate

that the structure is too complex to be fitted by a two-component model.

Hydra A.--Interpretation of the observed visibility curves for this source is difficult. There is a large, but faint halo with a diameter of about 5'. The core is certainly not circular; an elongation in a position angle of about 30° is indicated. It is possible that the core has an even more complicated structure; Lequeux and Heidmann (1961) find a very small-diameter component having about one-fifth the total intensity of the source at 21 cm.

M87.--This source was observed to have a core-and-halo type of structure by Biraud, Lequeux, and LeRoux (1960). A comparison of the 3-m observations by Mills (1953) and the observations at 21 cm by Biraud et al with the present measurements shows that the core is relatively less prominent at longer wavelengths (Moffet 1961). Over this range of wavelengths, the spectral index of the core is about -0.3, while the halo has a steeper spectrum with an index of about -1.0. Observations which we have made at 21.6 cm with a north-south antenna spacing of 1600 ft indicate that the core is elongated, with the major axis in a position angle of approximately 300° . This confirms the suggestion that the core is associated with the jet, which projects from the nucleus of the galaxy in position angle 290° (Baade and Minkowski 1954). Lequeux and Heidmann (1961) find that the core consists of two components with an east-west separation of 0.5 .

NGC 5128 (Centaurus A).--This source consists of an extended part with dimensions of about $3' \times 8'$ and a compact central core. The extended source has been shown to consist of two components (Bolton and Clark 1960; Wade 1959). Recent measurements by Twiss, Carter, and Little (1960) have shown that the central source also has two components. This result is confirmed by the present observations. Further investigations of the central source (Maltby 1961) have shown that the two components are elongated, with dimensions of about $3.8' \times 2.0'$. The components are separated by 7.1 ± 0.5 . The elongation is approximately in the direction of the major axis, and both components are situated well outside the wide dust band in NGC 5128.

There are two studies of the central source at other wavelengths in the decimeter range, both yielding information about the east-west brightness distribution. These studies are the previously mentioned one by Twiss, Carter, and Little (1960) at 21 cm and a recent one by Little and Bracewell¹ (1961) at 9 cm.

Table 2 lists some of the results of the three investigations. It is seen that at the longer wavelengths, the intensities and diameters of the two components are more nearly equal, and also the separation between them may be somewhat larger. A detailed comparison has been made between the east-west visibility function determined in Paper I and an artificial visibility function calculated for a model derived from the 9-cm observations. This comparison strengthens the suggestion that the structure of the source varies with wavelength. In particular, it is quite unlikely that the diameter of either component at 31 cm can be as small as 1'. The present measurements indicate that if the two components have unequal

¹We are indebted to Dr.'s Little and Bracewell for informing us of their results in advance of publication.

intensities the stronger lies toward the east, which is in agreement with the 9-cm result of Little and Bracewell.

Centaurus A was studied at a wavelength of 3 m by Mills (1953), using an interferometer with several baseline orientations and spacings. His results were difficult to interpret because of the presence of the extended source in his primary antenna pattern and because the phase of the visibility function was not measured. His results do not seem inconsistent with the interpretation given in Table 1; however his conclusion that the central source lies roughly in the dust lane of NGC 5128 would seem to be in error (Maltby 1961).

Hercules A.--The source consists of two components with an east-west separation of 1.92 ± 0.10 . The position angle of the major axis is 100.5 ± 1.0 , giving a separation of 1.95 along this axis. Observations at 21.6 cm with a north-south antenna spacing of 1600 ft have shown that the components are nearly circular in shape and have established the orientation of the major axis with this rather high degree of precision (see Figure 4). The east-west phase at the 779λ spacing (Paper I, Table 5) indicates that the stronger component is toward the east. The agreement with the results of Heidmann and Lequeux (1961) at 21 cm is excellent.

Cygnus A.--Measurements at Jodrell Bank have shown that at a wavelength of 2.4 m it appears to consist of two, roughly equal components (Jennison and Das Gupta 1953) and that it has a similar structure at 10 cm (Rowson 1959). Table 3 summarizes the results of the present work and of existing measurements at other wavelengths. It can be seen from Table 3 that as the wavelength of observation increases, the two components appear to draw closer together.

Jennison and Latham (1959) found that the two components of Cygnus A differed in intensity by 20% at 2.63 m, with the stronger component toward the west. This result was based on their phase measurements at antenna spacings of 1540λ and 2160λ east-west. In the present work, the phase measured at the 1557λ east-west spacing indicates a ratio of component intensities of 1.3 ± 0.3 to 1, but with the inequality in the opposite sense, i.e. with the stronger component toward the east¹. The phases reported by Twiss et al (1960) at 21 cm are in agreement with the 31 cm phases of Paper I. It would be desirable to have more complete and more precise measurements of the visibility phase in order to confirm this apparent variation of structure with wavelength.

c) Table of Galactic Sources

Table 4 contains information on 21 sources believed to lie within our own galaxy. For most of these sources the data on the visibility functions from Papers I and II were numerically inverted to give approximate one-dimensional brightness distributions. The diameter listed is in each case the angular distance between the half-intensity points of this distribution. For sources situated in the galactic plane, it is clear that our inversions do not present true pictures of the surrounding

¹The final intensity ratio of 1.2 ± 0.2 to 1 which is given in Table 1 is based on both the phase and amplitude data.

complex distribution of brightness¹. The reason is, of course, that the necessary brightness-distribution components of low spatial frequencies were not measured. Most of the sources listed in Table 4 have relatively sharp central concentrations, and the diameters listed are believed to be accurate.

Seven galactic sources were observed with both baselines. Of these, two were outside the limits of resolution of the instrument. The Supernova of 1572, the Crab and the Orion Nebulae, and probably Cass A showed rather similar diameters in the two directions, while 3C 58 showed a distinct elongation. In no case was there a clear division into well-separated components.

d) Distribution of the Sources

While various observers will doubtless find the descriptions of individual sources to be of value, the distribution of sources among the structural classes is perhaps of more general interest. This distribution is given in Table 5.

Appearing in Table 5 are 99 sources in class N, while 75 sources are distributed among the four well-resolved classes. These latter 75 are the sources for which some structural details could be determined. Of these, 60% were observed with both the north-south and the east-west baselines. Only in class S, the apparently simple sources, is the number found on the basis of observations with one baseline greater than the corresponding number for observations with both baselines. It is probable that several of the S sources observed with only one baseline actually have more-complicated structures. In addition, three of the four S sources observed with two baselines show a high degree of elongation, suggesting that they may be partially resolved double sources or double sources with the components partially superposed due to projection onto the plane of the sky. Only one source observed with both baselines displays a simple, roughly circular, one-component structure with a diameter >1.5 . This source is 3C 278². It seems safe to conclude that the relative number of simple, apparently circular extragalactic sources is quite small, perhaps smaller than 5%, but certainly smaller than 20%.

A great majority of the sources cannot be described by a single component and fall into classes H, U, or E. Most of these more-complicated sources have just two prominent components, superposed in class H and separated in classes U and E. A few sources which have been classified U or H may contain more than two components. For instance, in 3C 465 there is definite evidence for a halo, but there is also evidence for structure within the core. The core of Hydra A may likewise show structure³. In 3C 135, a very complex structure is indicated, but not defined, by the data available. The number of such well-resolved sources

¹See, for example, the 31-cm galactic maps of Wilson and Bolton (1960).

²In addition there are two sources in class N, 3C 78 and 3C 338, which show similar diameters of about 1' in two and three directions, respectively. These sources may likewise have simple structures.

³Recent work by Lequeux and Heidmann (1961) has revealed structure in the cores of both Hydra A and M87.

with more than two major components is not greater than 20, however, and may well be less. Thus, over half of the sources resolved in this study display structures consisting of two major components.

e) Two-Component Sources

Since so many of the sources appear to consist of two components, the properties of this group of objects were investigated in somewhat greater detail. More precisely, the properties of the class E and U sources were investigated; the class H sources seem to be a distinct group. In Figure 6 is shown a histogram of the numbers of sources from classes E and U displaying various ratios of component intensities. To make this histogram as complete as possible, the extended source in Centaurus A (Bolton and Clark 1960) and the source Fornax A (Wade 1961) have been added to the 34 sources for which intensity ratios are given in Table 1. Some sources with high intensity ratios have undoubtedly been overlooked in our interpretation, but the first three columns of the histogram are believed to be complete. There is an abundance of sources with components of approximately equal intensity as compared with those having intensity ratios in the range of 1.5 to at least 3.5. Although it is possible to modify the shape of this histogram somewhat by choosing different values for the column boundaries, the peak in the first column persists and is judged to be real.

The distribution of the axial ratios for the two-component sources was also investigated. This ratio was defined by the quotient of the major and minor diameters of a source, as nearly as these could be estimated. The orientation of a source must be at least approximately known in order to deduce values for the major and minor diameters; hence, only sources which had been observed with both baselines were considered. The median ratio for the 11 sources in class E was 3.3, with values ranging from 2.2 to 6. Often only a lower limit could be obtained for the class U sources, with values ranging from >2 to >10 . Again, however, a concentration in the neighborhood of 3 to 4 seems likely.

The high median value of the axial ratio makes possible the exclusion of one possible model for the two-component sources, namely a random distribution of isotropically radiating toruses. It can be argued that an optically thin torus seen edge-on would appear as a two-component source, since the optical depth at the extremities would be greater than that in the center. However, the median value of the axial ratio for such a distribution of toruses would lie between 1.3 and 2--the exact ratio depending on the relation of the thickness of the ring to its diameter. The median value of the axial ratio for the 15 sources in classes E and S is 3.2. Undoubtedly some of the sources from class U should be included in this group, but in no way could the median be brought below 2. The exclusion of the torus model is really a consequence of the extreme rarity of circular sources.

Several two-component sources stand out because of their large axial ratio and large angular spacing. Among these are 3C 62, 3C 89, and 3C 343. The separation is in each case $>10'$, with an axial ratio >10 . The source 3C 208 might also be an object of this type, although its angular spacing is only $6'$. Although these sources have high galactic latitudes, none has yet been identified with an optical object. According to current notions about optical identifications (Minkowski 1960; Bolton 1960), this suggests that these sources are at very great distances. The large angular diameter would then imply a large physical extent, perhaps as

great as several megaparsecs. This is indeed very large if such sources are to be associated with single galaxies. It is possible that such objects represent chance associations of small-diameter radio sources. It is also possible that they represent a distinct type of radio source, perhaps associated with a whole cluster of galaxies. At least in the case of 3C 89 there is fairly good positional agreement with a faint cluster of galaxies (T. A. Matthews, private communication). Because of their high axial ratios, these sources are very difficult to study with the interferometric techniques used in this investigation.

f) Source Brightness Temperatures

An attempt was made to calculate surface brightness temperatures for the extragalactic sources, using the brightness distribution information in Table 1 and the 31-cm fluxes from Papers I and II. The problem of obtaining useful brightness temperatures from the data at hand is made difficult by the complex nature of the sources. It has been customary to find a brightness temperature T_b from the relation

$$T_b \propto S / \left(\frac{1}{4} \pi d^2 \right) ,$$

where S is the observed flux from the source and d is the observed "diameter". It is clear from the results presented above that such a definition is not satisfactory for the large majority of radio sources; a complex source cannot be described by a simple diameter. A second approximation is to calculate mean brightness temperatures for the various components in a source. It is necessary to know the sizes and shapes of the individual components, which obviously requires greater resolution than is needed to distinguish the presence and rough relative positions of the components. For only a few sources were the data in Table 1 sufficient to calculate component brightness temperatures; the results are presented in Table 6. The figures not enclosed in parentheses are probably accurate to within a factor of two. Those enclosed in parentheses may be good only to an order of magnitude. Only for sources in class H are separate figures presented for the two components. Most of the brightness temperatures are between 10^3 and 10^4 °K, though the lowest is only 64°K (the halo of 3C 264) and the highest is 1.2×10^6 °K (Cygnus A). In M87 is seen a range of two orders of magnitude between the core and the halo. The range between the two sources in Centaurus A (NGC 5128) is even greater, since at this same wavelength Bolton and Clark (1960) found brightness temperatures in the extended source which give a mean of about 10^5 °K.

V. CONCLUSIONS

This investigation has greatly expanded the number of extragalactic radio sources for which some details of structure are known. It has shown that the great majority of these sources have complex structure, often with two prominent components. There is a tendency for these components to be rather symmetrical in intensity and size, though it is not clear that the very symmetrical sources (class E) form a truly distinct type. There is some evidence for a distinct group of sources, typified by 3C 89, with large axial ratios and often with unequal intensities. The small group of core-and-halo objects is important because it contains several intense sources having firm optical identifications (M87, Hydra A, and possibly NGC 1275).

A group of relatively small-diameter galactic radio sources was also investigated. Although these sources varied in complexity, they generally showed a more compact structure than that typical of the extragalactic sources.

A comparison of radio and optical brightness distributions for identified objects is naturally of great interest, and the fourth article in this series will be devoted to this subject. The optical identifications are particularly important because they offer a measure of the distance to the source. Given the distance, the angular dimensions can be changed into physical dimensions, and the energy requirements of the source can then be estimated. Since the complex nature of the sources has been demonstrated in the present paper, it seems appropriate to mention that there is no clear relation between radio and optical complexity in identified objects. A complex radio source can be associated with either a single or a multiple galaxy, while the source 3C 278, which has a simple radio structure, is associated with a double system, NGC 4782-83.

The fact that a radio source is typically elongated means that its angular extent must be specified by a major-axis diameter. The interferometric determination of this diameter requires measurements along at least two baselines. To determine a meaningful brightness temperature for a source, the sizes and shapes of the components must be known; this requires a higher order of accuracy and resolving power than does the initial resolution of the source into components.

A suggestion for further investigation comes from three extragalactic sources for which comparable studies have been made at other wavelengths, namely M87, NGC 5128, and Cygnus A. In each case the structure appears to vary with wavelength. It is not at all surprising that the core and the halo in M87 show different spectral characteristics, since the physical conditions in the two regions are almost certainly very different. The other sources in class H may show similar changes when observed at various wavelengths. The fact that a large proportion of the extragalactic sources--the ones with two well-separated components--have rather similar appearances at one wavelength suggests that the wavelength dependence of the structure in these sources may not be very great. The detection of small wavelength-dependent changes will require observations of great accuracy.

The fact that a radiogalaxy is typically complex and highly extended is presumably to be associated with the complex and powerful forces needed to bring such an object into being. A great deal of additional information will be required to permit an understanding of the origin and development of these objects. Much has been said about the cosmological significance of radio source statistics, but any cosmological conclusions will always be in doubt if the development of the sources themselves is not understood. The problem of the lifetime of a source is, for instance, very critical. The results of the present study suggest that an understanding of radio-source mechanisms may await the construction of radio telescopes having a degree of resolution comparable to that of present large optical telescopes.

VI. ACKNOWLEDGMENTS

The authors wish to thank G. J. Stanley, Director of the Observatory, for his interest in this work. One of us (P.M.) is the recipient of a Fulbright Travel Grant and a grant from the Norwegian Research Council for Science and the Humanities. The other (A.T.M.) has held a National Science Foundation Fellowship during the course of this work. The program of research in radio astronomy at the California Institute of Technology is supported by the United States Office of Naval Research under Contract Nonr 220(19).

TABLE 1

DIAMETERS AND COMMENTS ON STRUCTURE FOR THE EXTRAGALACTIC SOURCES

Source	Diameter		Class	Comments	
	p=90°	p=0°			
3C 2	< 0.5	< 0.5	N	Diameter in p=150° is 0.7±0.3. Diameter in p=150° is 1.1±0.4.	
3C 5	---	< 0.7	N		
MSH 00-29	---	< 1.0	N		
3C 15	1.2±0.5	< 0.6	N		
3C 17	1.5±0.5	< 0.5	N		
3C 18	---	1.1±0.2	N		
3C 19	---	< 0.5	N		
3C 20	< 0.7	< 0.5	N		
MSH 00-222*	---	5.0±2.0	(U)		
				Possibly 2 components, separation about 3' in p=0°. Diameter in p=150° is about 5', while the diameter in p=30° is somewhat larger.	
3C 23	---	< 1.0	N	Probably some structure present. Diameter in p=150° is 2.5±1.0.	
3C 26	< 0.7	< 0.7	N		
3C 27	---	0.5±0.3	N		
3C 28	< 0.7	< 0.8	N		
3C 29	---	2.5±0.7	(U)		
3C 32	---	< 0.8	N		
3C 33	C	C	U		
				2 components, relative intensities 2.5±0.7 and 1, separation 3.8±0.6 along major axis in p=20°±8°, with stronger component toward south-west. From 0 to 20% of the total flux could be in a third component near the centroid of the first two.	
3C 38	0.7±0.2	< 0.6	U	Probably 2 components, relative intensities 6±3 and 1, separation 5.0±1.0 in p=0°. Observations in p=150° agree with this interpretation.	
3C 40	C	C	U	2 components, relative intensities 3±1 and 1, separation 5.7±0.8 along major axis in p=129°±8°. Stronger component to south-east and probably extended in p=0°. Components < 1.2. Larger scale structure probable.	
3C 41	C	C	(U)		
3C 43	---	< 0.5	N	Possibly 2 components.	
3C 46	2.0±1.0	1.0±0.4	(U)		
3C 47	---	1.3±0.2	N		
3C 55	---	< 0.8	N		
MSH 01-315	---	< 1.4	N		
3C 62	---	C	U		
					2 components, relative intensities about 3 and 1. Possible separation is 11' in p=0°. Stronger component has diameter < 0.7.
3C 63	< 0.8	< 0.7	N		

TABLE 1 -continued

Source	Diameter		Class	Comments
	p=90°	p=0°		
3C 65	---	< 0.6	N	2 components, relative intensities 2.0±0.5 and 1, separation 6.6±1.0 along major axis in p=115°±7°, with stronger component toward south-east.
3C 66	C	C	U	
3C 69	---	0.8±0.2	N	2 components, equal intensities ±25%, equal diameters 1.2±0.2. Separation 2.8±0.4 along major axis in p=47°±7°.
MSH 02-110	< 1.0	< 0.5	N	
3C 71	< 0.5	< 0.5	N	
3C 75	C	C	E	
3C 78	1.0±0.5	1.0±0.3	N	4.5±1.0 halo with 15% of flux.
3C 79	1.2±0.3	< 0.7	N	
CTA 21	< 0.8	< 0.6	N	
NGC 1275*	< 0.7	0.7±0.3	(H)	
Fornax A *	> 20	> 20	U	2 components, relative intensities 4±1 and 1, separation 2.0±0.2 in p=0°.
3C 86	---	C	U	
3C 88	---	1.7±0.2	S	Probably 2 components, relative intensities about 3 and 1, separation about 6' in p=90° and about 8' in p=0°. Diameter of stronger component is < 1.0.
3C 89	C	C	U	
CTA 26	< 1.2	C	U	2 components, relative intensities 3±1 and 1, separation 2.3±0.5 in p=0°, with stronger component toward south.
MSH 03-19	---	2.0±0.3	S	2 components, relative intensities 3±1 and 1, separation 3.4±0.5 along major axis in p=25°±10°, with stronger component toward north-east.
MSH 03-212	---	3.0±0.7	S	
3C 98	C	C	U	
3C 103	< 0.5	C	E	2 components, equal intensities ±25%, diameters < 1.0, separation 1.3±0.2 in p=0°.
3C 105	---	C	H	5.0±1.0 halo and < 1.0 core with about 50% of flux.
MSH 04-12	---	0.8±0.3	N	2 components, equal intensities ±15%, equal diameters 1.2±0.3, separation 2.5±0.3 along major axis in p=60°±7°.
3C 109	< 1.0	1.3±0.3	N	
MSH 04-24	---	1.0±0.4	N	
3C 111	C	C	E	
3C 119	---	< 0.5	N	Standard source, except at the largest antenna spacing in p=0°.
MSH 04-112	---	2.5±0.5	S	
3C 123	< 0.4	0.5±0.2	N	

TABLE 1 -continued

Source	Diameter		Class	Comments
	p=90°	p=0°		
MSH 04-218 3C 129	--- C	1.5±0.3 2.5±0.4	N (U)	Diameter in p=150° is 1.5±0.5. Considerable structure, components < 1.0. 2 components of comparable intensity indicated in p=0°. Overall diameter ≥ 6' in p=90°.
3C 131	---	< 0.6	N	Possibly a halo with 20 % of flux. Probably weak companion about 8.5 away in p=0°, relative intensities ≈ 5 and 1.
3C 132	---	< 0.8	N	
3C 133	---	< 1.0	U	
3C 134 *	0.6±0.2	C	E	2 components, equal intensities ±15%, separation 2.0±0.2 along major axis in p=175°±5°. The components are elongated approximately along the major axis with diameter 0.5x1.0 each.
MSH 05-13 3C 135	--- C	< 1.5 C	N (U)	Considerable structure, overall diameter ≥ 4', fine structure < 1.0. Structure present in p=90°.
Pictor A *	7.5±1.0	< 2.0	(U)	Diameter in p=36° and p=144° is < 1.0. Standard source.
3C 138	---	< 0.5	N	
MSH 05-36	---	< 1.0	N	
3C 141	---	1.0±0.5	N	Standard source.
3C 147	< 0.4	< 0.4	N	
3C 153	---	< 0.5	N	
3C 154	0.6±0.3	< 0.5	N	
3C 158	---	< 0.8	N	
3C 159	---	< 0.9	N	
3C 161	< 0.4	0.5±0.3	N	
3C 166	---	0.5±0.3	N	
3C 171	< 0.7	< 0.6	N	
MSH 06-216 3C 172	--- ---	< 0.8 C	N E	
3C 175	0.7±0.3	< 0.7	N	
3C 178	---	< 1.0	N	
3C 180	< 1.0	2.0±0.5	(S)	
3C 184	---	< 0.9	N	
3C 187	---	C	U	
MSH 07-117	---	C	U	2 components, relative intensities 2.5±1 and 1, separation 1.9±0.2 in p=0°, with stronger component toward south. Overall diameter ≥ 3', fine structure < 1.0.
3C 191	< 0.7	< 0.6	N	Standard source.
3C 192	---	1.6±0.3	S	
3C 195	---	1.5±0.4	N	
3C 196	< 0.4	< 0.4	N	

TABLE 1 -continued

Source	Diameter		Class	Comments
	$p=90^\circ$	$p=0^\circ$		
3C 198	3.5 ± 1.0	3.5 ± 1.0	H	Observations in $p=90^\circ$ indicate < 1.5 core with $\approx 25\%$ of flux. Observations in $p=30^\circ$ and $p=150^\circ$ indicate that the halo is nearly circular.
3C 202	---	0.7 ± 0.3	N	2 components, relative intensities 4 ± 1 and 1, stronger source has diameter < 1.0 . Separation 6.1 ± 0.7 along major axis in $p=138^\circ \pm 7^\circ$, with stronger component toward north-west.
3C 208	C	C	U	
3C 212	---	< 0.7	N	About $5'$ halo with $12\% \pm 5\%$ of flux. Core diameter ≈ 1.2 in $p=30^\circ$ and < 0.6 in $p=90^\circ$ and $p=150^\circ$.
MSH 08-219	---	< 0.7	N	
3C 216	< 0.6	< 0.6	N	
Hydra A*	1.0 ± 0.5	1.5 ± 0.7	H	
3C 219	C	C	E	2 components, equal intensities $\pm 20\%$, equal diameters 0.85 ± 0.15 , separation 1.9 ± 0.1 along major axis in $p=35^\circ \pm 3^\circ$.
3C 225	---	1.0 ± 0.7	U	Structure, components < 1.0 .
3C 227	2.8 ± 0.5	0.6 ± 0.4	U	2 components, relative intensities 2 ± 1 and 1, separation 2.1 ± 0.5 along major axis in $p=90^\circ \pm 10^\circ$. The components are probably elongated along the major axis.
3C 228	---	0.8 ± 0.2	N	Structure, principal component < 1.0 . Overall diameter about 3.0 , with principal component < 1.0 .
3C 230	C	1.0 ± 0.3	(U)	
3C 234	C	0.7 ± 0.3	(U)	
3C 237	< 0.6	0.5 ± 0.3	N	Considerable structure, principal component < 1.0 . Diameter ≈ 3.0 in $p=142^\circ$.
3C 238	---	C	(U)	
MSH 10-44	---	< 2.0	N	2 components, relative intensities 2 ± 1 and 1, diameter < 1.0 each, separation 2.0 ± 0.3 in $p=0^\circ$. Possible larger-scale structure.
3C 243	C	C	U	
3C 245	---	< 1.0	N	Halo diameter > 6.0 , core diameter < 1.2 with about 60% of flux.
3C 254	< 0.5	< 0.5	N	
MSH 11-18	---	< 0.5	N	
3C 261	---	< 0.8	N	
3C 264	2.0 ± 1.0	2.0 ± 1.0	H	
3C 265	1.2 ± 0.3	< 0.7	N	
3C 267	---	< 0.7	N	2 components, equal intensities $\pm 15\%$, equal diameters 2.7 ± 0.5 , separation 4.7 ± 0.3 along major axis in $p=85^\circ \pm 7^\circ$.
3C 270	C	2.5 ± 0.5	E	
3C 273	< 0.4	< 0.4	N	

TABLE 1 -continued

Source	Diameter		Class	Comments
	$p=90^\circ$	$p=0^\circ$		
M 87*	C	C	H	6.5 ± 0.7 halo with $48\% \pm 3\%$ of flux, core diameter is 0.6 ± 0.2 . The core is elongated in $p \approx 300^\circ$.
M 84	---	1.8 ± 1.0	N	
3C 275	---	< 0.7	N	
Coma A	< 0.8	< 0.7	N	
3C 278	2.5 ± 0.5	2.0 ± 0.5	S	Diameter is 2.0 ± 0.5 in $p=31^\circ$ and $p=149^\circ$. The source is nearly circular.
3C 279	< 0.6	< 0.6	N	
3C 280	< 0.6	< 0.5	N	
3C 283	< 0.7	< 0.7	N	
NGC 5128* (center source)	C	C	E	2 components, equal intensities $\pm 30\%$, separation 7.1 ± 0.5 along major axis in $p=46.5 \pm 2^\circ$. One or both components are elongated in $p \approx 15^\circ$ ---diameters 3.8×2.0 .
3C 287	< 0.8	< 0.6	N	
3C 286	< 0.4	< 0.4	N	
MSH 13-33	---	4.0 ± 0.5	S	
MSH 13-011	---	< 0.7	N	
3C 295	< 0.4	< 0.4	N	Standard source.
3C 298	< 0.5	< 0.5	N	
MSH 14-011	---	< 1.0	(U)	Large scale structure possible.
MSH 14+010	C	C	(U)	Large scale structure, principal component < 1.0 .
MSH 14-121	---	0.7 ± 0.3	N	
3C 310	1.8 ± 0.3	C	(E)	Probably 2 components, equal intensities $\pm 15\%$, equal diameters 2.0 ± 0.5 , separation 2.1 ± 0.2 in $p=0^\circ$.
3C 313	C	1.6 ± 0.3	U	2 components, relative intensities 1.6 ± 0.4 and 1, diameters < 1.0 , separation 1.9 ± 0.2 along major axis in $p=56^\circ \pm 7^\circ$, with stronger component toward south-west.
3C 315	1.0 ± 0.2	1.5 ± 0.3	(S)	
3C 317	< 0.5	0.6 ± 0.2	N	
3C 318	< 0.6	< 0.6	N	
3C 324	< 0.7	< 0.7	N	
3C 327	C	0.7 ± 0.3	U	2 components, unequal intensities or diameters, separation 3.5 ± 0.5 in $p=90^\circ$. Components apparently elongated in $p=90^\circ$.
MSH 16+02	< 0.7	< 1.0	N	
3C 330	1.2 ± 0.2	---	(S)	
3C 338	1.2 ± 0.2	---	N	Diameters in $p=43^\circ$ and $p=137^\circ$ are 1.1 ± 0.3 . The source is nearly circular.

TABLE 1 -continued

Source	Diameter		Class	Comments
	$p=90^\circ$	$p=0^\circ$		
3C 343	C	---	E	2 components, equal intensities $\pm 30\%$, both diameters < 0.7 , separation in $p=90^\circ$ certainly $\geq 6'$, possible separation $11'$.
3C 345	< 0.7	---	N	
3C 347	C	---	U	Possibly 2 components, relative intensities 3 ± 1 and 1, both diameters < 1.0 . Separation 2.9 ± 0.6 in $p=90^\circ$.
Herc. A*	C	C	E	2 components, relative intensities 1.4 ± 0.1 and 1, equal diameters 0.75 ± 0.20 , separation 1.95 ± 0.10 along major axis in $p=100^\circ 5' \pm 1.5$. Stronger component probably toward east.
3C 353	C	---	U	2 components, relative intensities 2.0 ± 0.3 and 1, equal diameters 1.4 ± 0.2 , separation 2.5 ± 0.1 in $p=90^\circ$, with stronger component toward east.
3C 365	< 2.0	---	(U)	Possibly complex structure with components < 0.7 .
3C 380	< 0.4	---	N	
CTA 80	2.0 ± 0.5	---	U	Highly elongated, probably 2 components of unequal intensity, separation 1.7 ± 0.4 along major axis in $p=55^\circ \pm 15^\circ$.
3C 386	1.9 ± 0.2	---	(S)	Slight central concentration.
3C 388	< 0.8	---	(U)	Possibly a faint (about 10%) component 3.5 away in $p=90^\circ$.
MSH 19-16	< 1.5	---	N	
3C 401	< 0.5	---	N	
3C 402	2.0 ± 0.5	---	U	Possibly 2 components, diameter < 1.0 each, separation 1.5 ± 0.3 in $p=90^\circ$.
3C 403	C	---	E	2 components, relative intensities 1.2 ± 0.2 and 1, equal diameters 1.2 ± 0.3 , separation 1.56 ± 0.15 in $p=90^\circ$.
Cygnus A*	C	0.8 ± 0.2	E	2 components, relative intensities 1.2 ± 0.2 and 1, equal diameters 0.7 ± 0.2 , separation 1.58 ± 0.10 along major axis in $p=109^\circ \pm 1.5$. Possible elongation of components in direction of major axis.
3C 409	< 0.5	---	N	
3C 410	< 0.5	---	N	
3C 413	C	---	(E)	Probably 2 components, equal intensities $\pm 60\%$, separation 1.7 ± 0.3 in $p=90^\circ$.
3C 424	< 0.6	---	N	
3C 430	0.6 ± 0.3	---	N	

TABLE 1 -concluded

Source	Diameter		Class	Comments
	$p=90^\circ$	$p=0^\circ$		
3C 433	< 0.5	0.6 ± 0.2	N	Probable large scale structure.
3C 436	< 1.0	1.6 ± 0.5	N	
3C 438	< 0.5	< 0.5	N	
3C 441	---	0.7 ± 0.3	N	
3C 442	---	3.0 ± 1.0	S	
3C 444	0.6 ± 0.3	2.0 ± 0.5	(S)	
3C 445	1.6 ± 0.3	C	(E)	
3C 446	C	< 0.8	U	Highly elongated. Probably 2 components, equal intensities $\pm 15\%$, equal diameters 1.5 ± 0.5 , separation 3.8 ± 0.4 in $p=0^\circ$. Probably 2 components, relative intensities 6 ± 2 and 1, separation 1.8 ± 0.3 in $p=90^\circ$.
CTA 102	< 0.6	< 0.6	N	Considerable structure.
3C 452	4.0 ± 2.0	1.2 ± 0.2	(U)	
3C 456	C	C	U	
3C 459	< 0.7	< 0.8	N	Complex structure, components < 1.0 .
MSH 23-112	< 0.8	< 1.2	N	
3C 465	C	C	(H)	
3C 469	< 1.2	< 1.5	N	Overall diameter 5.0 ± 1.0 , components < 1.0 .

Table 2

FEATURES OF NGC 5128 OBSERVED AT DIFFERENT WAVELENGTHS

Wavelength	E-W Component Separation	Relative Component Intensities	E-W Component Diameters
31 cm	$5'.1 \pm 0'.4$	$<1.3:1$	$2'.4 \pm 0'.4$ each
21 cm	5'	---	2'.5 each
9 cm	4'.6	1.8:1	$2'.6 \pm 0'.2$ and $<1'$

Table 3

FEATURES OF CYGNUS A OBSERVED AT DIFFERENT WAVELENGTHS

Wavelength	Observing Group	Reference	E-W Component Separation	Position Angle of Major Axis
2.63 m	Jodrell Bank	(a)	1'.35	97°
31.3 cm	Caltech	---	$1'.49 \pm 0'.12$	$109^\circ \pm 1^\circ 5''$
21.1 cm	Nancay	(b)	1'.52*	---
21.0 cm	Sydney	(c)	1'.47*	
10.7 cm	Jodrell Bank	(d)	1'.59*	$109^\circ \pm 2^\circ$

(a) Jennison and Latham (1959).

(b) Biraud et al (1960).

(c) Twiss et al (1960).

(d) Rowson (1959).

* Inferred from minimum in published curves of visibility amplitude.

** Position angle determined from measurements at 21.6 cm.

TABLE 4

DIAMETERS AND COMMENTS ON STRUCTURE FOR THE GALACTIC SOURCES

Source	Diameter		Comments
	$p=90^\circ$	$p=0^\circ$	
CTA 1	---	$>20'$	Probably a ring-shaped source.
S.N. 1572	6.0 ± 2.0	7.0 ± 1.0	
CTA 6	---	>20	
3C 48	<0.4	<0.4	Standard source in $p=0^\circ$.
3C 58	6.0 ± 1.0	2.3 ± 0.3	Some fine structure.
Crab. Neb.	3.3 ± 0.4	3.7 ± 0.4	Nearly Gaussian distribution in $p=90^\circ$; less central concentration in $p=0^\circ$.
Orion Neb.	4.1 ± 0.4	4.8 ± 0.4	Central concentration, extended to- wards south.
IC 443	---	>20	Approximately 65% of flux in $\approx 10'$ halo, core diameter 1.8 ± 0.4 .
Rosette Neb.	---	>20	
Puppis A	>15	>20	
CTB 31	C	---	
CTB 32	1.4 ± 0.4	---	Central concentration.
CTB 38	C	---	Complex structure, overall diameter $>8'$ with components $<3'$.
S.N. 1604	3.0 ± 0.4	---	Considerable small-scale structure.
Sagr. A	C	---	20% $\pm 5\%$ of flux in 2.2 ± 0.5 core. Halo diameter $\approx 12'$.
Omega Neb.	4.5 ± 0.6	---	Slightly asymmetrical.
3C 397	2.0 ± 0.5	---	Complex halo with diameter $\approx 10'$.
3C 398	2.1 ± 0.5	---	Complex halo with diameter $\approx 6'$.
CTB 87	3.8 ± 0.5	---	
CTA 97	10 ± 3	---	
Cass. A	>3.5	3.8 ± 0.5	Less centrally concentrated than a Gaussian distribution.

Table 5

CLASSIFICATION OF THE 174 EXTRAGALACTIC SOURCES

Classification	E	U	H	S	Total of Resolved Sources	N	Total of All Sources
Observed with two baselines	11	24	6	4	45	45	90
Observed with only one baseline	4	16	1	9	30	54	84
Total observed	15	40	7	13	75	99	174

Table 6

MEAN COMPONENT BRIGHTNESS TEMPERATURES AT 31.3 CM

Source	Class	T_b ($^{\circ}$ K)	Source	Class	T_b ($^{\circ}$ K)	Source	Class	T_b ($^{\circ}$ K)
3C 33	U	(20,000)	3C 198	H	120+(> 200)	NGC 5128	E	15,000
3C 40	U	(2,000)	Hydra A	H	1700+(20,000)	Center		
3C 46	(U)	(500)	3C 219	E	4,000	3C 310	(E)	900
3C 66	U	(30,000)	3C 227	U	(5,000)	3C 315	(S)	(2,000)
3C 75	E	1500	3C 264	H	64+(> 2000)	3C 327	U	(5,000)
3C 111	E	4000	3C 270	E	1,000	Herc A	E	40,000
3C 134	E	8000	M 87	H	2000+2x10 ⁵	Cyg A	E	1.2x10 ⁶
Pictor A	(U)	(3000)	3C 278	S	1200	3C 445	(E)	(1,000)

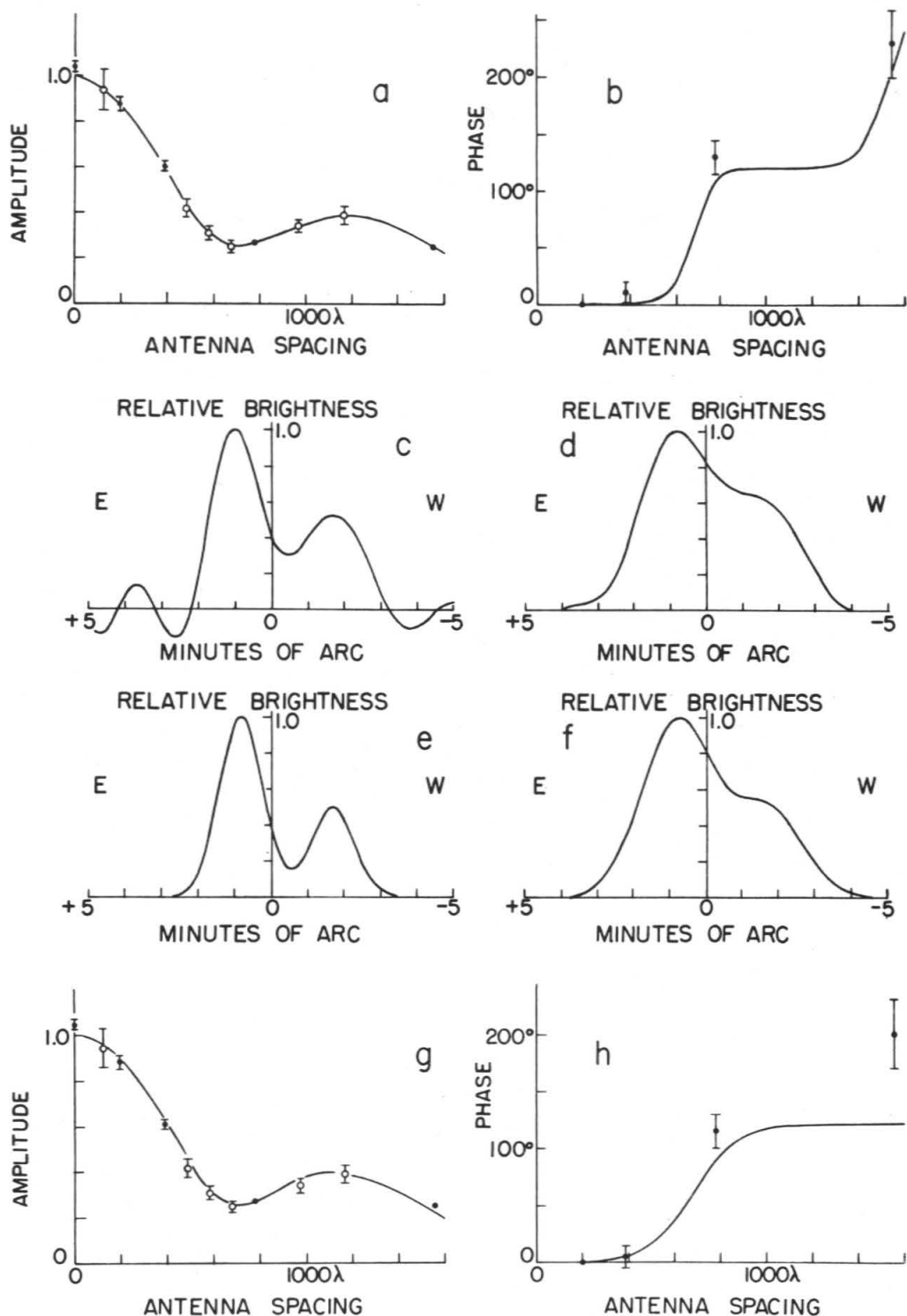


Fig. 1. Interpretation of the source 3C 353. a. Visibility amplitude. b. Visibility phase. c. Principal solution obtained by inversion of a and b. d. Principal solution smoothed with a 1.8 Gaussian. e. Source model made up of two 1.4 Gaussians, relative intensities 2.0 and 1, spacing 2.5. f. The same model, but smoothed with a 1.8 Gaussian. g and h. The observed points compared with the calculated amplitude and phase for the model shown in e.

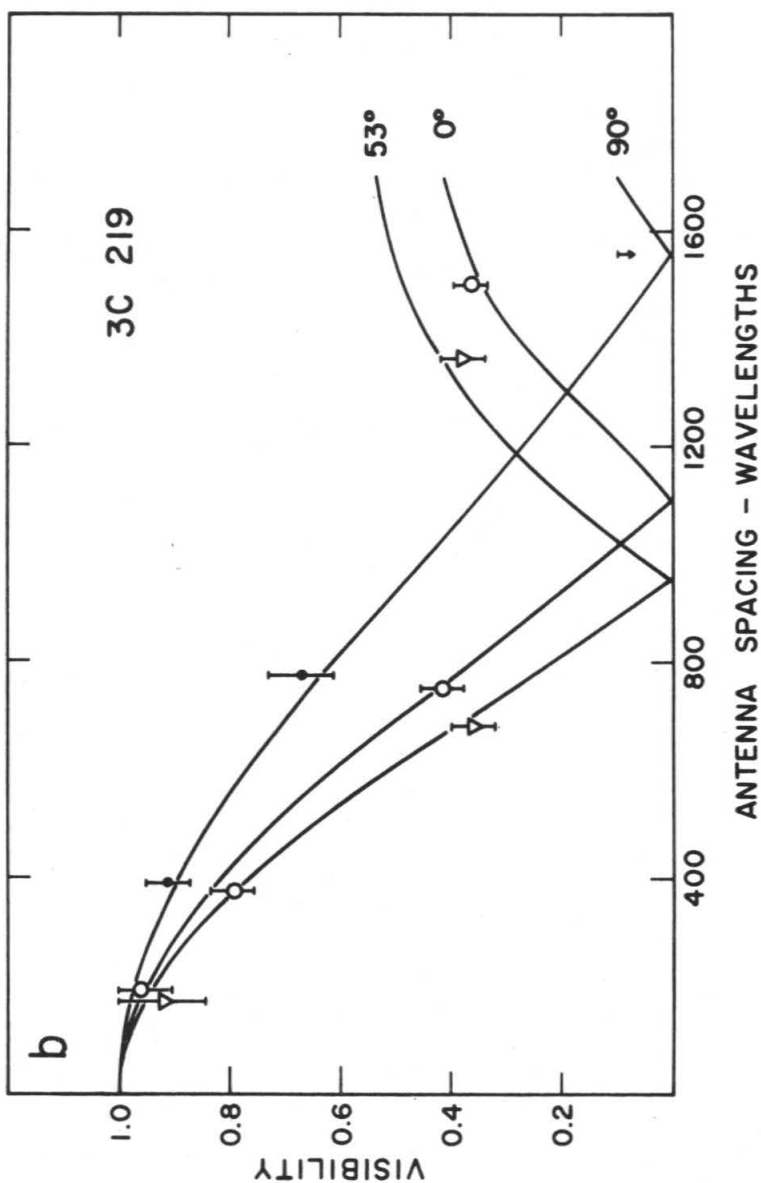
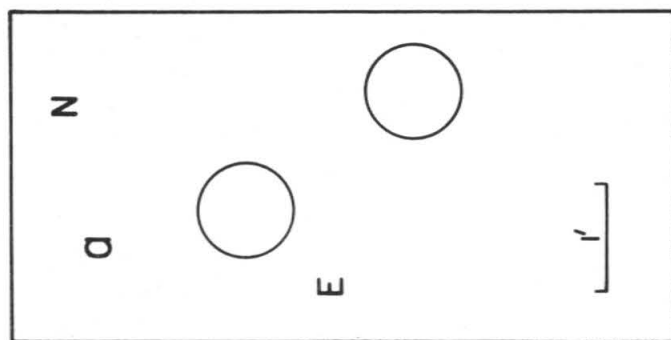


Fig. 2. a. Model for 3C 219. b. Comparison of observed visibility amplitudes with the curves calculated from the model.

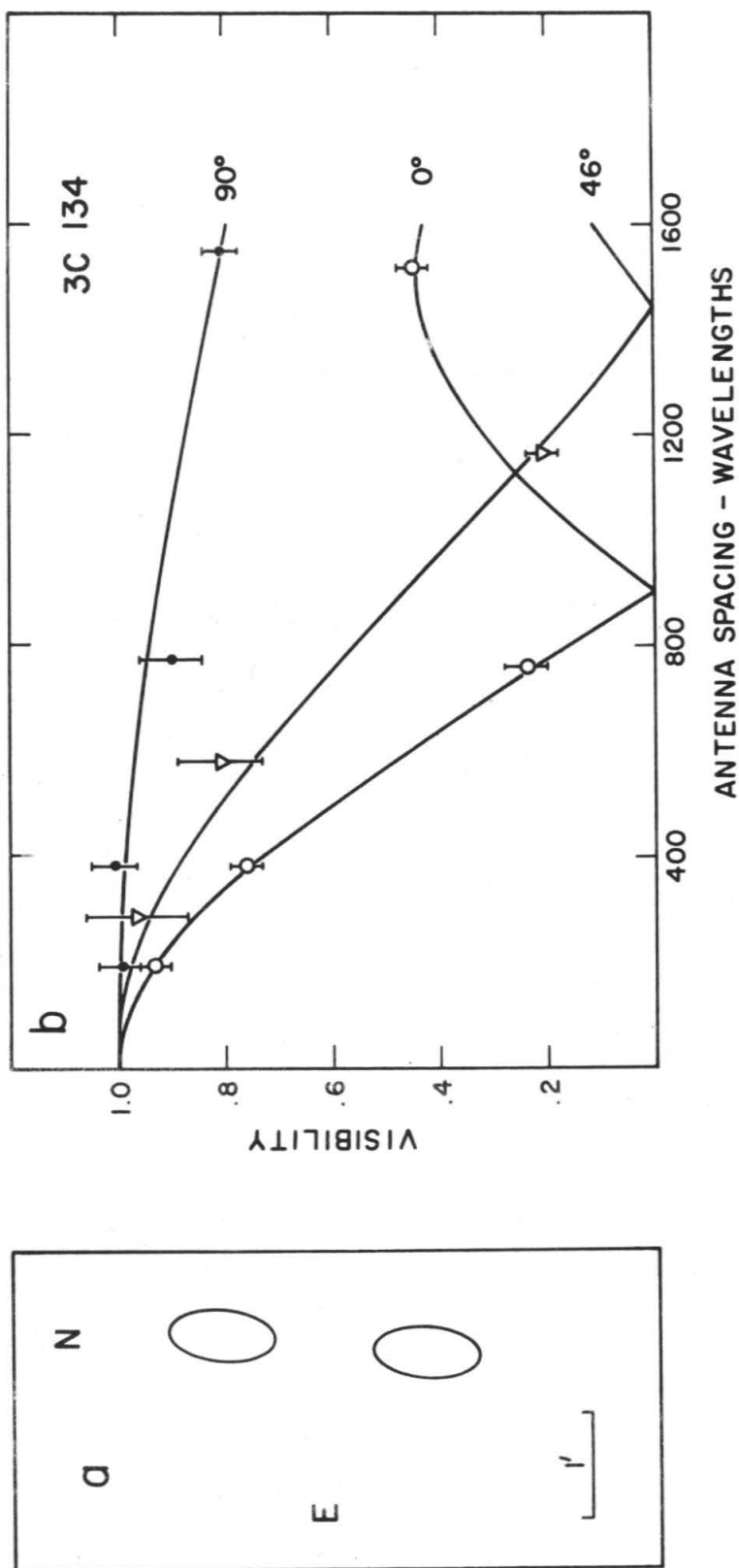


Fig. 3. a. Model for 3C 134. b. Comparison of observed visibility amplitudes with the curves calculated from the model.

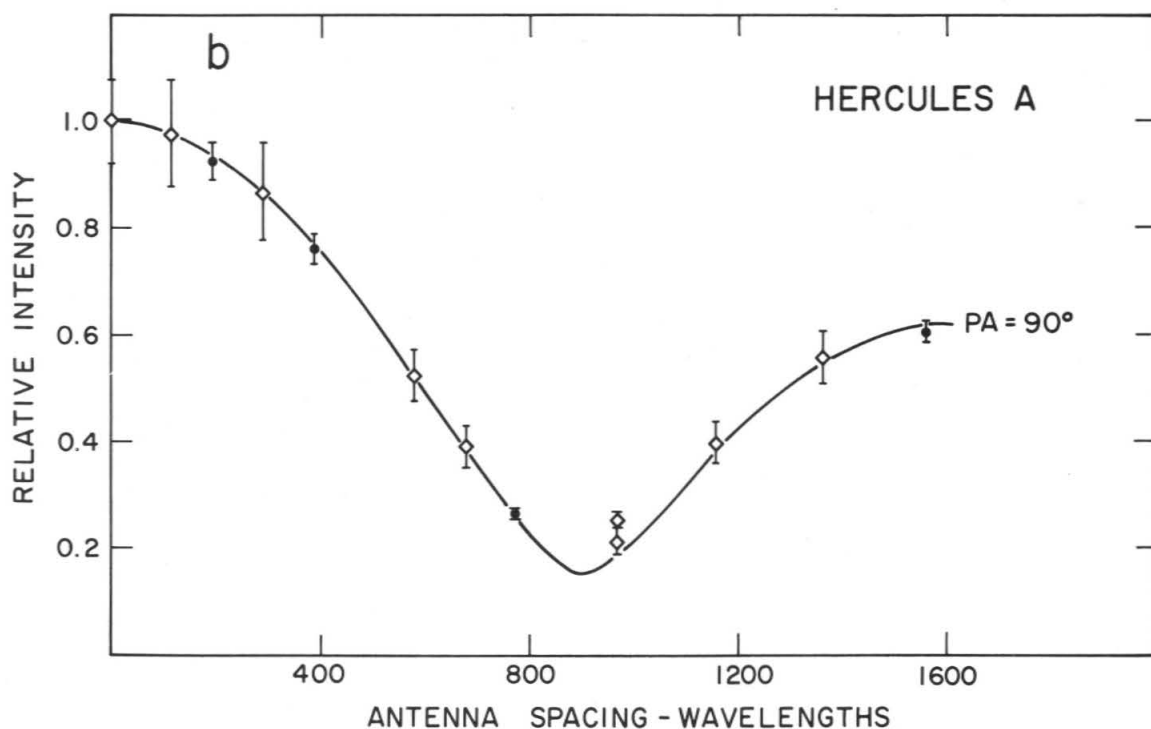
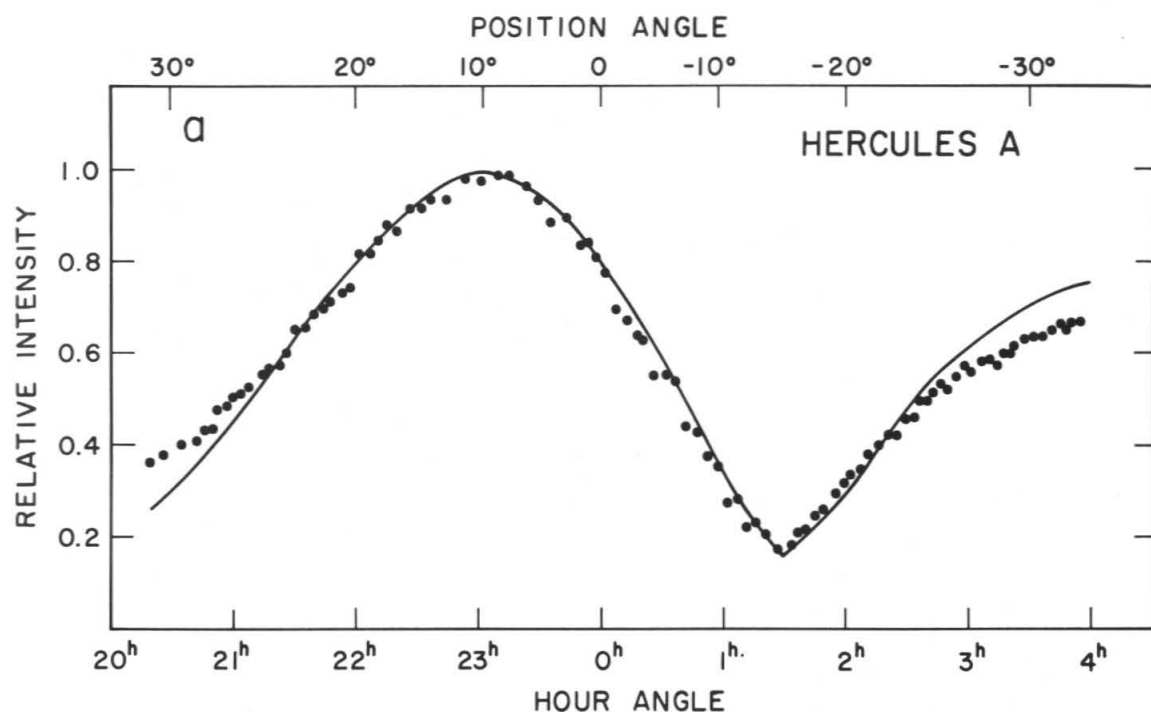


Fig. 4. a. Visibility amplitudes observed for Hercules A while tracking with a long north-south baseline. The curve is calculated for the model described in Table 1. b. Comparison of observed east-west visibility amplitudes with the curve calculated for the model.

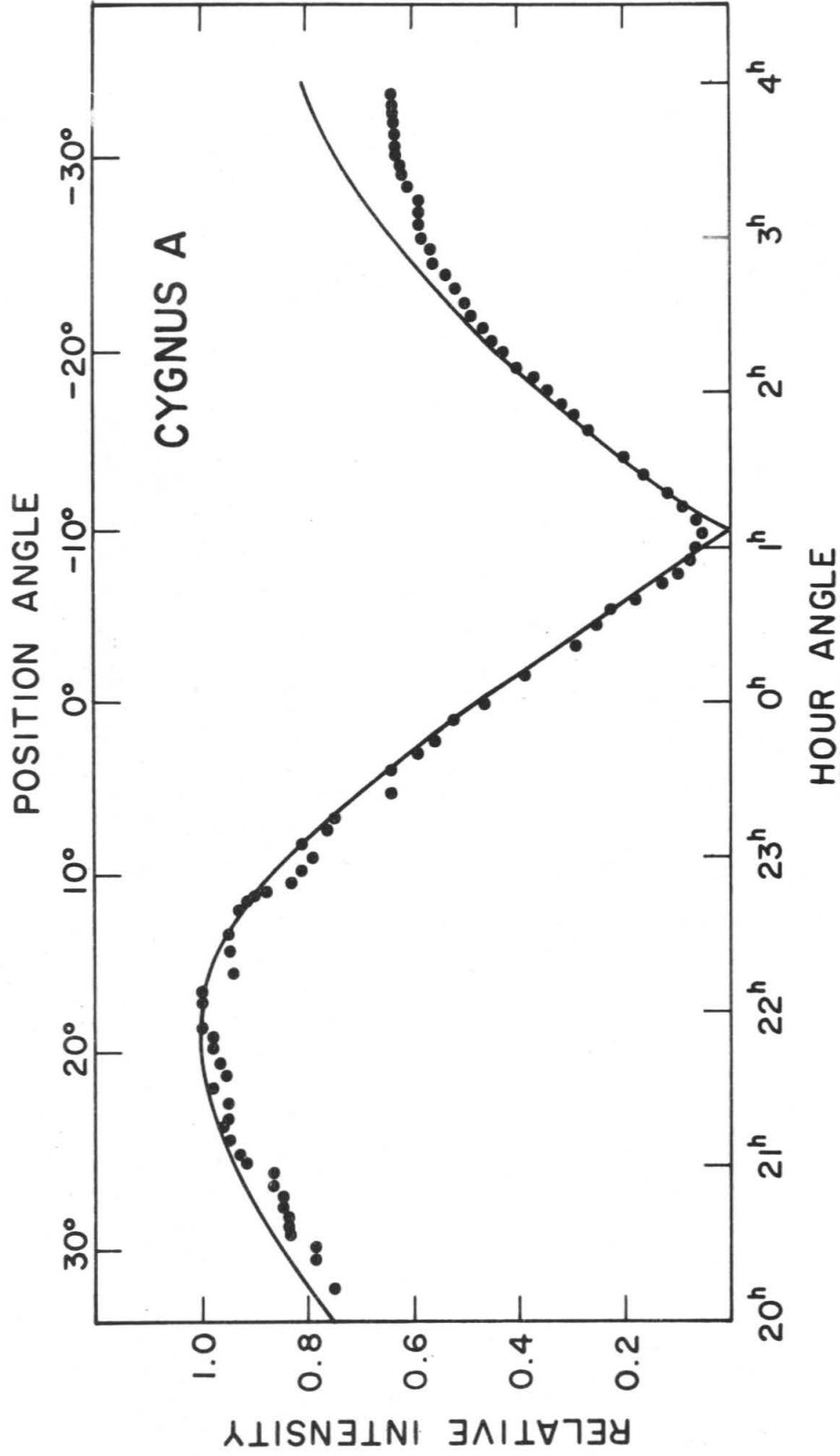


Fig. 5. Visibility amplitudes observed for Cygnus A while tracking with a long north-south baseline. The curve is calculated for the model described in Table 1. The departure after $HA = 2 \frac{1}{2}h$ may indicate an elongation of the components in the direction of the major axis.

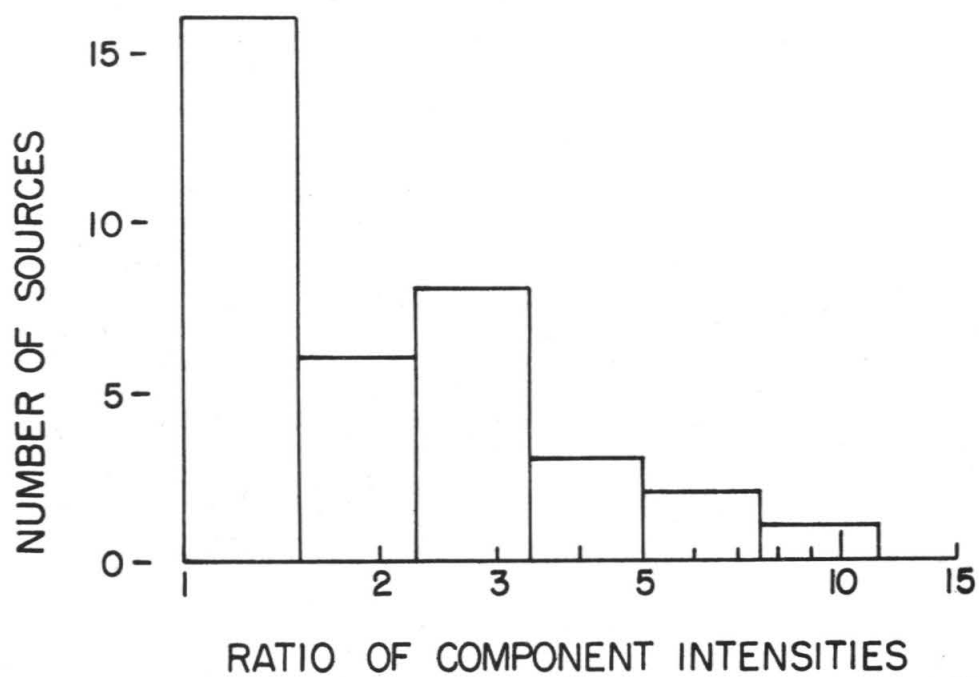


Fig. 6. Number of sources versus the ratio of the component intensities.

REFERENCES

- Baade, W., and Minkowski, R. 1954, Ap. J., 119, 215.
- Biraud, F., Lequeux, J., and LeRoux, E. 1960, Observatory, 80, 116.
- Bolton, J. G. 1960, Introductory talk at the session on discrete sources, U.R.S.I. General Assembly, London; also 1960, Obs. Calif. Inst. of Tech., 5.
- Bolton, J. G., and Clark, B. G. 1960, Pub. A.S.P., 72, 29.
- Bracewell, R. N., and Roberts, J. A. 1954, Australian J. Phys., 7, 615.
- Heidmann, J., and Lequeux, J. 1961, Compt. rend., 253, 226.
- Humason, M. L., Mayall, N. U., and Sandage, A. R. 1956, A.J., 61, 97.
- Jennison, R. C., and Das Gupta, M. K. 1953, Nature, 172, 996.
- Jennison, R. C., and Latham, V. 1959, M. N., 119, 174.
- Lequeux, J., and Heidmann, J. 1961, Compt. rend., 253, 804.
- Leslie, P. R. R., and Elsmore, B. 1961, Observatory, 81, 14.
- Little, A. G., and Bracewell, R. N. 1961, A. J., 66, 290.
- Maltby, P. 1961, Nature, 191, 793.
- Maltby, P. 1962, Ap. J. Suppl., ____.
- Maltby, P., Matthews, T. A., and Moffet, A. T. 1962, Ap. J. Suppl., ____.
- Mills, B. Y. 1953, Australian J. Phys., 6, 452.
- Minkowski, R. 1960, Proc. Natl. Acad. Sci. U. S., 46, 13.
- Moffet, A. T. 1961, A. J., 66, 49.
- Moffet, A. T. 1962, Ap. J. Suppl., ____.
- Rowson, B. 1959, M. N., 119, 26.
- Twiss, R. Q., Carter, A. W. L., and Little, A. G. 1960, Observatory, 80, 153.
- Wade, C. M. 1959, Australian J. Phys., 12, 471.
- Wade, C. M. 1961, Pub. Natl. Radio Astron. Obs., 1, 99.
- Wilson, R. W., and Bolton, J. G. 1960, Pub. A. S. P., 72, 331.